Proposed Contribution, 15th ASME Wind Energy Symposium,
Houston, Texas, Jan. 28–Feb. 2, 1996

Fatigue Design of Wind Turbine Blades: Load and Resistance Factors from Limited Data

Clifford H. Lange and Steven R. Winterstein
Civil Engineering Dept., Stanford University

Abstract

This paper considers the design of wind turbine blades to resist fatigue failures. It shows new models to reflect the impact of limited information, and applies these to several cases with notably different amounts of loads data. In each case separate load and resistance factors are developed for fatigue-resistant design. When load data are abundant, reliability is found to be driven almost solely by the resistance; e.g., by the conservatism implied in the design S–N curve. The case of sparse-load data is found to yield roughly equal contributions from load and resistance uncertainty, suggesting roughly equal conservatism should be assigned to load and resistance factors.

Introduction

This paper considers the design of wind turbine blades to resist fatigue failures. In particular, separate load and resistance factors are developed for load and resistance factor design (LRFD) against fatigue. The use of separate load and resistance factors is consistent with a wide range of current, probability-based design codes (e.g., API, 1993).

This paper combines several novel approaches to the blade fatigue problem. These include (1) the use of FORM/SORM (first- and second-order reliability methods) to estimate failure probabilities and dominant uncertainty sources (e.g., Veers et al, 1993); (2) new moment-based model of wind turbine loads, designed especially to reflect limited load data (e.g., Winterstein and Lange, 1995); and (3) a parallel LRFD study of a specific Danish wind turbine, also based on FORM/SORM (Ronold et al, 1994).

Scope and Organization

The dominant fatigue blade loading is assumed here to be flapwise bending. We consider the following 3 different horizontal-axis wind turbines (HAWTs), for which measured load data are available.

Turbine 1 is the AWT-26 machine, a downwind, two-bladed, free-yaw turbine with teetered rotor, with rotor diameter of 26m and power rating of 275kW (McCoy, 1995). This turbine is used for our base case study, in view of the relatively large amount of load data available (197 10-minute segments).

Turbine 2 is an upwind, two-bladed HAWT with a rotor diameter of 17.8m and a power rating of 100kW, operated by Northern Power Systems (Coleman and McNiff, 1989). It has a teetering hub design with full-span hydraulic passive pitch control. It affords a contrast to Turbine 1 both in mechanical design, and in the amount of available load data (only 20 10-minute segments).

Turbine 3 is a Danish machine, with hub height of 35m and power rating of 500kW. This has been the subject of a similar LRFD study on wind turbine blade fatigue (Ronold et al, 1994). This study has been supported as one of four sub-projects within the 1994–1995 European Wind Turbine Standards (EWTS) project.

We seek here both to demonstrate basic methodology for fatigue reliability, and to identify the general impact of different load models on reliability calculations. We thus consider normalized bending loads from these various turbines, and fit different probability distributions to each. To focus on load modelling only, we adopt the same, hypothetical models of wind environment and blade properties in each case. Thus, our results are not intended to apply specifically to any of the machines in question. Rather, they should be seen as the result of applying various plausible load

models to the same (hypothetical) wind turbine blade.

Background: Probabilistic Design

1. Probabilistic Design against Overloads.

Historically, codified probabilistic design has been most widely applied to "overload" failures, caused when the worst load in the service life of a component, L, exceeds its capacity R. If both the load L and resistance R were known perfectly at the time of design, we would merely require that $R \geq L$. More generally, in load- and resistance-factor design (LRFD) separate factors, γ_L and ϕ_R, are used to scale the nominal load and resistance, L_{nom} and R_{nom}:

$$\phi_R R_{nom} \geq \gamma_L L_{nom} \tag{1}$$

Of course, in any single situation Eq. 1 can be replaced by a checking equation involving a single design factor SF_{des} on the net safety factor:

$$SF_{nom} = \frac{R_{nom}}{L_{nom}} \geq SF_{des}\,; \quad SF_{des} = \frac{\gamma_L}{\phi_R} \tag{2}$$

With the two factors γ_L and ϕ_R, however, Eq. 1 can more readily give uniform reliability across various cases—specifically, covering cases in which uncertainty in load may dominate over that of resistance, or vice versa. Similarly, different factors may be applied to separate load contributions which show different variability. Examples include separate factors for dead and live loads on offshore structures (API, 1993), or the separate factors recently suggested for static, wave-frequency, and slow-drift loads on floating structures (Banon et al, 1994).

2. Probabilistic Design against Fatigue

Because fatigue is the cumulative result of many loads, the choice of an "equivalent" load L and resistance R is somewhat ambiguous. Fatigue predictions are generally based on tests with constant stress amplitude S (and mean stress S_m=0). The resulting number of cycles to fail, $N(S)$, is commonly modelled with a power-law relation:

$$N(S) = N_{ref} S_{norm}^{-b}\,; \quad S_{norm} = \frac{S}{S_{ref}} \tag{3}$$

Here S_{ref} is a reference stress level, and N_{ref} the number of cycles to fail at that level. Both N_{ref} and the power-law exponent, b, are material properties, both of which may generally be considered uncertain. Miner's rule then assigns damage D=$1/N(S)$ per cycle, and hence average damage $\overline{D}$=$\overline{S_{norm}^b}/N_{ref}$ over the service life of the specimen. (Overbars are used here to denote average values.) More generally, this damage rate $\overline{D}$ can be adjusted to reflect (1) a stress concentration factor K relating local to far-field stresses; (2) an availability factor A, the fraction of time the wind turbine component operates; and (3) the effect of a non-zero mean stress S_m, which with the Goodman rule scales the fatigue life by $(1 - KS_m)/S_u$ (here S_u=ultimate stress). This results in the effective damage rate

$$\overline{D}_{eff} = \frac{\overline{S_{norm}^b}}{N_{eff}}\,; \quad N_{eff} = N_{ref} \frac{(1 - KS_m/S_u)^b}{AK^b} \tag{4}$$

Finally, we can identify load and resistance variables, L and R, such that $L \geq R$ implies fatigue failure. If we seek the specimen to withstand N_{ser} cycles in its service life, Miner's rule predicts failure if $\overline{D}_{eff} N_{ser} \geq 1$. Here we generalize this failure criterion to read $\overline{D}_{eff} N_{ser} \geq \Delta$; randomness in Δ reflects possible errors (both bias and uncertainty) in Miner's rule. This implies a failure criterion of the form $L \geq R$, in terms of the following "fatigue" load and resistance:

$$L = \overline{S_{norm}^b} \cdot N_{ser}\,; \quad R = N_{eff} \cdot \Delta \tag{5}$$

Note that in this formulation, fatigue load and resistance have units of cycles. (Alternative formulations can instead assign load and resistance factors γ'_L and γ'_R in terms of stresses; e.g., Ronold et al, 1994. Numerical values of these factors may differ notably; we may expect $\gamma'_L \approx \gamma_L^{1/b}$ because damage is related here to the b-th power of stress.) Our current formulation seeks to reflect common usage; e.g., a nominal value of N_{eff} may be based on a lower-fractile S–N curve. The resulting load factor γ_L serves to inflate a number of load cycles to be withstood; for example, critical offshore facilities are often designed against γ_L=10 times the service life (e.g., demonstration of 200-year nominal life if the actual service life is 20 years).

We seek below to (1) model load variability given limited wind and load data; (2) study sensitivity to various modelling assumptions, different machines, etc.; and (3) suggest convenient choices of nominal fatigue load and resistance, and associated load and resistance factors γ_L and ϕ_R, to achieve desired reliability against fatigue failure.

Fatigue Loads for Given Wind Climate

A central thesis of our ongoing work on fatigue load modelling is that smooth, analytical probability distributions are conveniently fit to a limited number

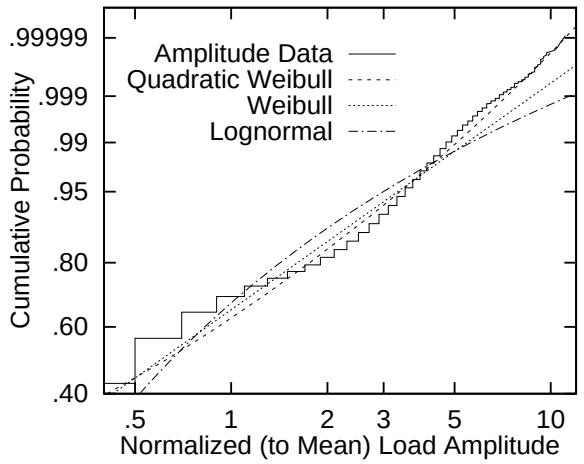

Figure 1: Distribution of normalized loads (Turbine 1: $V = 11.5$ m/sec, $I = .16$).

of statistical moments (e.g., Winterstein and Lange, 1995). We work here with the first three moments, defined as follows:

$$\mu_1 = \overline{S} \tag{6}$$

$$\mu_2 = \frac{\sigma_S}{\mu_1}; \quad \sigma_S^2 = \overline{(S-\overline{S})^2} \tag{7}$$

$$\mu_3 = \frac{\overline{(S-\overline{S})^3}}{\sigma_S^3} \tag{8}$$

Note that both μ_2, the coefficient of variation, and μ_3, the skewness coefficient, are normalized to be unitless. Successively higher moments provide increasingly detailed information about rare large loads, at the expense of being increasingly difficult to estimate from limited data. Alternatively, one may estimate the b-th moment (and hence $\overline{S_{norm}^b}$) directly from data, thus avoiding the need to fit any theoretical probability model. Our use of lower-moment models, however, seeks to reduce the variability associated with estimating $\overline{S_{norm}^b}$, particularly for the relatively high b values (e.g., 10 or above) found for some composite materials (e.g., Mandell et al, 1993).

Following common wind turbine practice, we divide load histories into 10-minute segments. Rainflow-counted stress ranges, S, are identified for each segment, and the results binned by mean wind speed V and turbulence intensity I. Figure 1 shows a resulting distribution of flapwise bending loads, found for Turbine 1 at a wind climate bin centered at V=11.5 m/s and I=.16. This is a fairly frequently occurring bin, and Figure 1 reflects a total of roughly 5 hours of data. The results are shown on "Weibull scale," along which any Weibull model of the form

$$\text{Prob [load } > s] = \exp[-(s/\beta)^\alpha] \tag{9}$$

will appear as a straight line. Special cases include the exponential (α=1) and Rayleigh (α=2) models. Both of these have been previously applied to model HAWT and VAWT loads (Jackson, 1992; Kelley, 1995; Malcolm, 1990; Veers, 1982).

The Weibull model in Figure 1, fit to the first two moments μ_1 and μ_2, appears to match the data fairly well. It fails, however, to reflect the systematic curvature the data display on this scale. An alternate two-moment model, the lognormal, is shown to induce curvature in the other direction, suggesting it notably overestimates loads at high-fractile levels. (A 4-moment variation on this lognormal model has been used in the Danish wind turbine study of Ronold et al, 1994.)

We also show results from a "quadratic Weibull" model, based on the first three moments of the data. It begins with the Weibull model S_{weib} of Figure 1, fit to μ_1 and μ_2. If the skewness μ_3 of the data exceeds that of S_{weib}, a quadratic term is added to S_{weib} to broaden its probability distribution:

$$S = s_{min} + \kappa[S_{weib} + \epsilon S_{weib}^2] \tag{10}$$

When the skewness μ_3 of the data is less than that of S_{weib}, the roles of S and S_{weib} in Eq. 10 are interchanged:

$$S_{weib} = s_{min} + \kappa[S + \epsilon S^2] \tag{11}$$

(This quadratic equation is readily inverted to yield an explicit result for S in terms of S_{weib}.) In either case, the fitting proceeds in 3 steps: (1) ϵ is chosen to preserve the skewness, μ_3; (2) κ is chosen to recover the correct variance, σ_S^2; and (3) the shift parameter s_{min} is finally introduced to recover the correct mean, μ_1. Note that our previous work (Winterstein and Lange, 1995) and subroutine `FITTING` (Winterstein et al, 1994) have also included a cubic term in Eqs. 10–11, thus permitting a four-moment fit. Our subsequent experience suggests that three-moment models may well suffice for fatigue load ranges; moreover, they avoid the need to solve simultaneous nonlinear equations to preserve both the third and fourth moments.

Figure 1 shows that the quadratic Weibull model indeed provides an improved fit to the data. Note here that the best Weibull model, S_{weib}, overestimates the frequency of large loads, and hence the load skewness. Thus we select Eq. 11, with $\epsilon > 0$ to ensure that S has narrower distribution tails than S_{weib}. Similar trends are found for this turbine in other wind conditions, as shown in the next section.

Fatigue Loads Across Wind Climates

To implement the preceding 3-moment load model for various wind conditions, best estimates E[μ_i] ("expected values") of the three moments μ_i (i=1,2,3) have been found for each V–I bin. The following power-law relation has then been fit:

$$\mathrm{E}[\mu_i] = a_{oi}(\frac{V}{V_{ref}})^{a_{1i}}(\frac{I}{I_{ref}})^{a_{2i}} \qquad (12)$$

Figures 2–4 show resulting estimates of E[μ_i] for the three wind turbines. (All loads have been normalized by their respective mean values at V=V_{ref}=7.5m/s, so that all results in Figure 2 predict unit values of the normalized mean load at V=V_{ref}.) Note that all results are shown versus mean wind speed V at a reference turbulence intensity I=I_{ref}=0.15. Because all quantities showed relatively moderate variation with I, this dependence is not shown in the figures (although it is kept in the subsequent analyses).

Most notable in these figures is the similarity of the various turbines: Turbines 1 and 2 show similar estimates of all 3 moments, and Turbine 3 gives consistent μ_1 and μ_2 (albeit apparently lower μ_3 estimates). In this regard, note that Turbine 3 results are inferred from cited results (Ronold et al, 1994) for the mean μ'_1, standard deviation μ'_2, and skewness μ'_3 of S'=ln S. Figures 2–7 have been constructed from Taylor series approximations, which suggest the mean load $\mu_1 \approx \exp(\mu'_1)$, while the higher unitless moments $\mu_i \approx \mu'_i$ for i=2 and 3. These approximations may add to the discrepancy, however, for example in Figure 4.

In general, Figure 3 suggests that for all 3 turbines, the coefficient of variation μ_2 generally exceeds 1.0, its value for an exponential model. Thus the "best" two-moment Weibull model is broader in its tail, or more damaging, than the commonly used exponential. However, the skewness μ_3 is generally less than 2.0, the corresponding value for an exponential variable. This implies that the basic Weibull fit, while more damaging than a body-fit exponential, in turn overestimates damage due to large load levels. In other words, the result shown in Figure 1 for Turbine 1 is symptomatic of various turbines in diverse wind climates: the data show curvature on Weibull scale, toward lower load levels at high fractiles than the Weibull model predicts. This effect will grow in importance as the fatigue exponent b increases; e.g., as we move from common metals to composites.

Analogous to Eq. 12, power-law fits have also been made of the corresponding standard deviations, D[μ_i], of the 3 moments $\mu_1 ... \mu_3$. These have been estimated for each V–I bin by a bootstrapping technique, in which "equally likely" rainflow range data (the same number as observed) are found by resampling from the observed ranges. These quantities D[μ_i] directly reflect the impact of limited data, and approach zero as the amount of data grows. We should thus expect cases with little data (e.g., Turbine 2) to show relatively higher uncertainty levels, D[μ_i], than those with more data (Turbines 1 and 3). Again Turbines 1 and 2 are found to yield consistent results in Figures 5–7. Turbine 3 appears relatively more variable, especially in Figures 5–6 and at extreme wind speeds. It is not clear whether this reflects the observed data for this turbine, our approximation of moments of S from those reported of ln S, or the extrapolation of functional forms beyond the range of observed data.

Fatigue Reliability Results

From Eq. 5, the fatigue loading involves the b-th moment $\overline{S^b_{norm}}$=$\overline{S^b}/S^b_{ref}$. This weights the conditional moment $\overline{S^b|V,I}$, given various values of V and I, by their joint probability density $p(V,I)$:

$$\overline{S^b} = \int\int_{all\ V\ I} \overline{S^b|V,I} \cdot p(V,I) dV dI \qquad (13)$$

We assume here that the mean wind speed V has Weibull distribution, with average $\overline{V}$ and shape parameter α_V. The turbulence intensity I is assumed independent of V, and assigned lognormal distribution with average $\overline{I}$ and coefficient of variation COV_I. Finally, we estimate $\overline{S^b|V,I}$ from three moment-based fits: the Weibull, lognormal, and quadratic Weibull models as in Figure 1. From the previous section, the necessary moments μ_i are modelled as

$$\mu_i = \mathrm{E}[\mu_i] + \mathrm{D}[\mu_i] \cdot U_i\ ; \quad i = 1,2,3 \qquad (14)$$

in terms of standard normal variables U_i. Correlations among the U_i are included, estimated from all the moment data irrespective of their V and I values. This approach directly parallels that suggested in the Danish fatigue reliability study (Ronold et al, 1994).

Thus, the fatigue load L=$\overline{S^b} \cdot N_{ser}/S^b_{ref}$ is modelled here as a function of 7 uncertain quantities:

$$L = L(\boldsymbol{X}) = \frac{\overline{S^b}(\boldsymbol{X}) \cdot N_{ser}}{S^b_{ref}} \qquad (15)$$

in which $\boldsymbol{X}$=[$\alpha_V, \overline{V}, COV_I, \overline{I}, U_1, U_2, U_3$]. Table 1 shows the distribution types and parameters for each of these variables, as well as of the net resistance variable $R = N_{eff} \cdot \Delta$ in Eq. 5. (Generally, this would in turn require joint modelling of its various components; e.g., N_{ref}, K, S_m, S_u, and A in Eq. 4; cf Veers

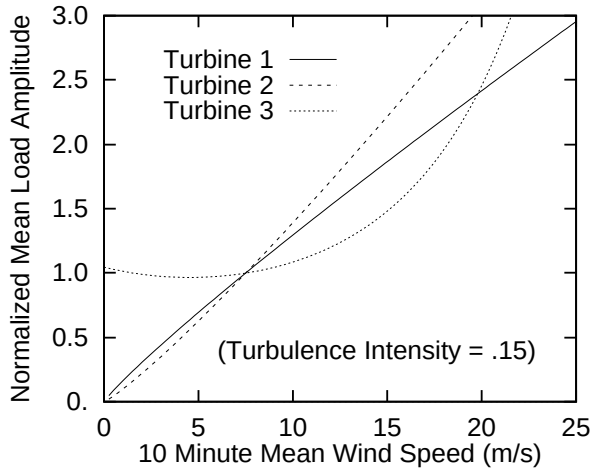

Figure 2: Estimated mean of normalized loads.

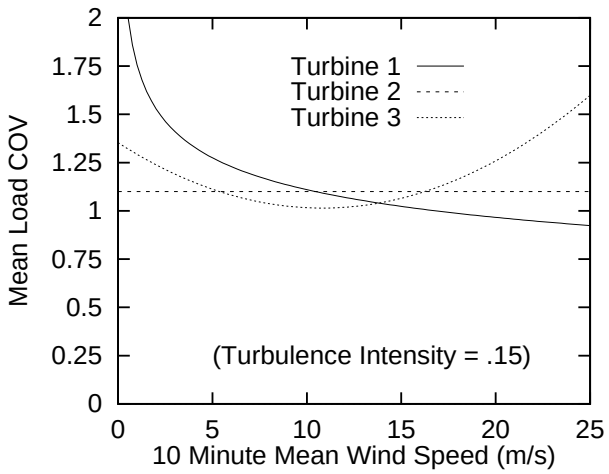

Figure 3: Estimated load coefficient of variation (COV).

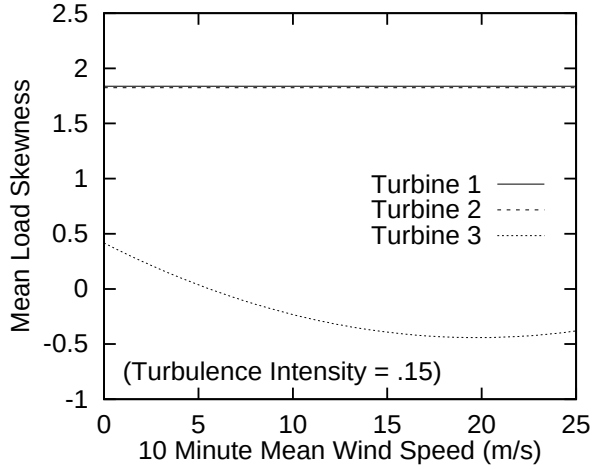

Figure 4: Estimated load skewness.

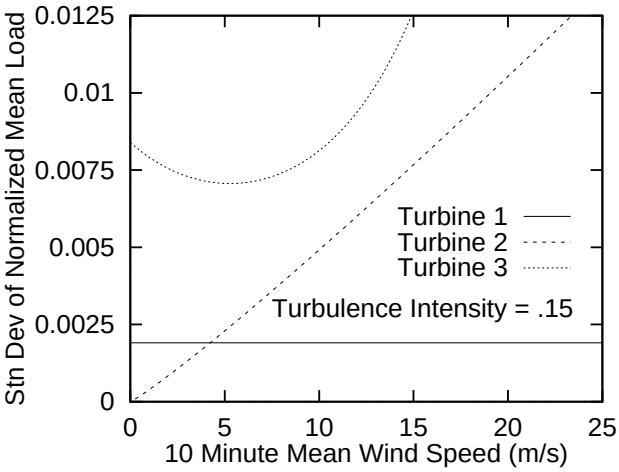

Figure 5: Standard deviation, estimated mean load.

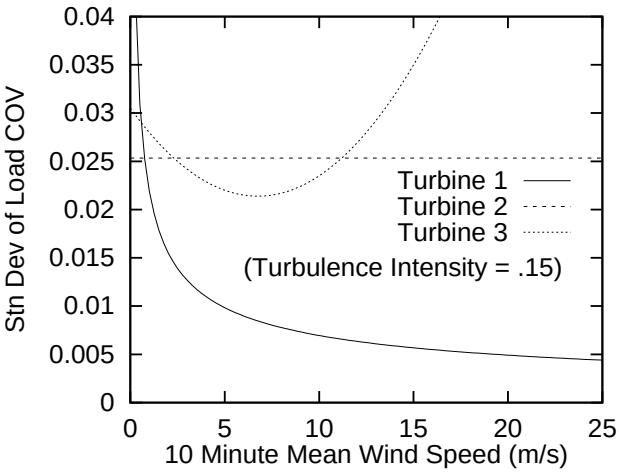

Figure 6: Standard deviation, estimated load COV.

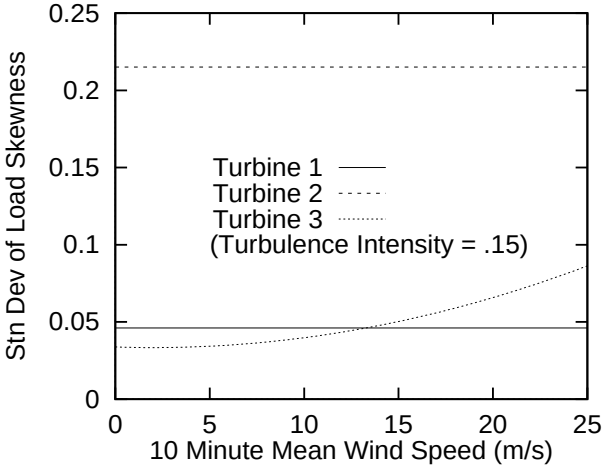

Figure 7: Standard deviation, estimated load skewness.

Variable	Distribution	Mean	Stn Dev
α_V	Weibull	1.8	0.135
$\overline{V}$	Normal	7.5	0.563
COV_I	Weibull	0.25	0.019
$\overline{I}$	Normal	0.15	0.011
U_1	Normal	0.0	1.0
U_2	Normal	0.0	1.0
U_3	Normal	0.0	1.0
R	Weibull	2.42E+18	1.69E+17
N_{ser}	Constant	4.10E+09	-
b	Constant	8.0	-

Table 1: Random variables in reliability analyses.

	Stress Distribution Type		
	Log	Weibull	Quad Weib
p_f:	4×10^{-4}	4×10^{-4}	5×10^{-4}
Variable	Uncertainty Percentage		
α_V	0.0	0.6	2.7
$\overline{V}$	0.1	1.6	3.3
COV_I	0.2	0.0	0.0
$\overline{I}$	2.6	1.2	1.0
U_1	0.1	0.0	0.2
U_2	0.6	0.1	0.0
U_3	-	-	0.3
R	96.4	96.6	92.5

Table 2: Turbine 1 reliability results; all results with same normalized fatigue load L_{nom}.

et al, 1993. Here, however, for simplicity we choose the value b=8 and the resistance variable R to have net coefficient of variation of 0.70.)

Variations with Load Distribution

We first consider results for Turbine 1, comparing the effect of switching between the three load models as in Figure 1: lognormal, Weibull, and quadratic Weibull. As in Figure 1, we pursue moment-based fits, matching μ_1 and μ_2 for the two-parameter models, and μ_1 through μ_3 for the quadratic Weibull. Thus all three models yield identical fatigue damage results for fatigue exponents b=1 and 2; the quadratic Weibull would also agree with the observed damage when b=3.

With the exponent b=8 chosen here, however, these models yield dramatically different estimates of fatigue damage, and hence of the probability p_f of fatigue failure within 20 years (N_{ser}=4.1 $\times$ 10^9 cycles at an average rate of 6.5 Hz). Typical p_f values differ by more than 5 orders of magnitude: from less than 10^{-6} to above 10^{-1}.

This highlights the importance of choosing an appropriate load model. It reflects the well-known effect of tail-sensitivity in reliability: while the first two moments of S have been preserved here, the higher moment $\overline{S^b}$ can vary greatly among various models fit to the same data. This effect grows with b; note that we choose here b=8, which is a relatively high value for metals but relatively low for many composites.

Redesign to Reflect Load Distribution

The foregoing shows that if we consider an identically designed turbine blade, its fatigue reliability is altered notably by the choice of load distribution. Conversely, vastly different load factors would be needed to achieve the same reliability for different load distributions—i.e., much higher load factors if the lognormal model were correct, much lower for the Weibull model, and so forth.

To reduce this sensitivity of load factors to distribution choice, we can seek to reflect the load distribution type in our nominal load. Assume we consider a design parameter W, which relates the observed bending moment M to resulting stress S; i.e., S=M/W. We may then seek to adjust W to preserve the mean damage, given our best estimates of the distributions of V, I and $S|V,I$—in other words, choose W to preserve

$$L_{nom} = \overline{S^b_{norm}} \cdot N_{ser} = L(\boldsymbol{X} \text{ given } X_i = \overline{X_i}) \quad (16)$$

Thus, if applied moments M truly follow a lognormal model we would require a sturdier blade—i.e., higher W to preserve $\overline{S^b}$=$\overline{M^b}/W^b$—than if a Weibull model of M were correct. Moreover, these differences between blade designs would increase with b, to reflect increasing sensitivity to distribution choice as b grows. Other design rules are also possible; e.g., choose W to preserve a specific upper fractile of the long-run stress distribution. An advantage of preserving L_{nom} in Eq. 16, however, is that it reflects not only the choice of load distribution but also the fatigue material behavior (i.e., choice of b).

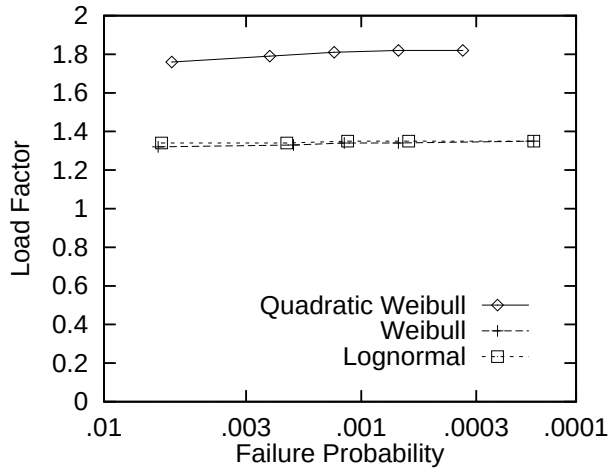

Figure 8: Load factors, Turbine 1.

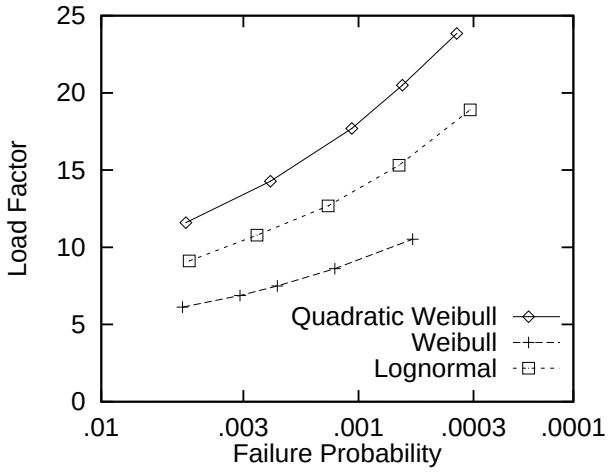

Figure 10: Load factors, Turbine 2.

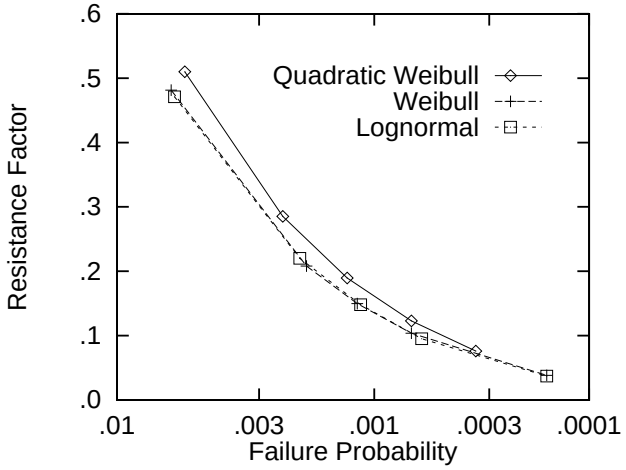

Figure 9: Resistance factors, Turbine 1.

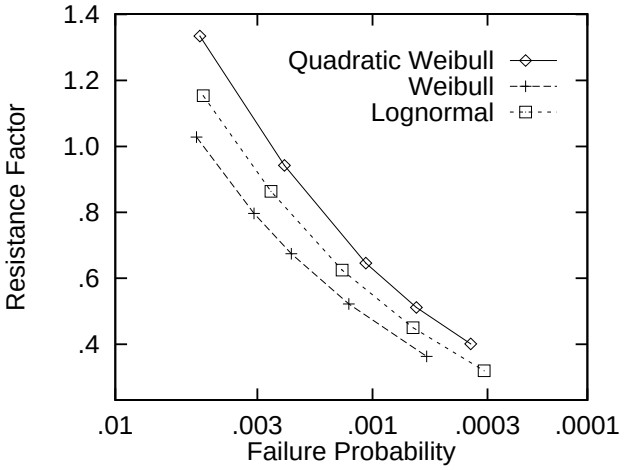

Figure 11: Resistance factors, Turbine 2.

Table 2 shows the resulting advantage of the nominal load definition in Eq. 16. By redesigning the component in each case to preserve the nominal load L_{nom} in Eq. 16, the results are only mildly sensitive to the choice of load distribution. In fact both two-moment models (lognormal and Weibull) give p_f=4 $\times$ 10^{-4}, with almost all uncertainty due to N_{eff} (96–97%). The three-moment model (quadratic Weibull) gives slightly higher p_f, due to the additional uncertainty in the higher-moment statistic μ_3. (The uncertainy contribution of N_{eff} is thus reduced to 92.5% in this case.)

We therefore suggest that load factors γ_L should be based on the nominal load defined in Eq. 16. This should promote relatively stable results across different materials and load modelling assumptions.

LRFD Results: Turbine 1

Finally, we consider the inverse problem of probabilistic design: what factors γ_L and ϕ_R should be used in Eq. 1, with nominal fatigue load L_{nom} and resistance R_{nom}, to achieve a target failure probability p_f over the service life? Here FORM/SORM methods are particularly useful. In addition to providing estimates of p_f and uncertainty contributions, they provide most likely load and resistance values, L^* and R^*, to cause failure at the design lifetime. By setting our design load and resistance to these most likely values, we can estimate the necessary factors:

$$\gamma_L = L^*/L_{nom}\,; \quad \phi_R = R^*/R_{nom} \qquad (17)$$

Regarding nominal loads and resistances, we again

use Eq. 16 to define a "mean" nominal load L_{nom}. Recall that L_{nom} has units of "cycles" so that corresponding load factors are applied to an expected number of service lifetime cycles. In contrast, following common practice the nominal fatigue resistance, R_{nom}, is set at its lower 2.3% fractile, i.e., the underlying normal variable lies two standard deviations below the mean. Figures 8–9 show resulting load and resistance factors, respectively, for Turbine 1. As may be expected, the resistance factor ϕ_R decreases steadily as the target p_f is lowered, and is always less than 1 for the p_f range shown. This reflects that while the nominal resistance R_{nom} was somewhat conservatively set (2.3% fractile), still lower resistances must be designed against if we require still rarer failure events.

Note from Figure 8, however, that the required load factor γ_L is effectively constant over the several decades of p_f values shown. This is because load uncertainty is relatively unimportant in this case. (Recall this is the case of relatively dense load data; the uncertainty contributions from all 7 wind and load variables remains less than 7.5% throughout.) The actual load factor γ_L is not 1.0, however; somewhat larger values (γ_L=1.4–1.8) are needed to cover not the uncertainty in load, but rather the *bias* between the nominal "mean" load L_{nom} and the actual load L^* most likely to cause failure.

LRFD Results: Turbine 2

Figures 10–11 show analogous load and resistance factors for Turbine 2. Results vary markedly from those for Turbine 1. Due to the relatively sparse load data in this case, FORM results show roughly equal contribution from load and resistance uncertainty. As a result, the implied load and resistance factors in Figures 10–11 vary similarly over the range of p_f values reported: γ_L varies by about a factor of 2, and ϕ_R by about a factor of 3. Note also that for relatively high p_f values, the 2.3% fractile nominal resistance R_{nom} is too conservative; ϕ_R factors above 1.0 show that we may design with a less conservative S–N curve. However, to cover load uncertainty we may need γ_L on the order of 10; i.e., ensure that our design life is an order of magnitude greater than the service life.

Finally, note again that our formulation applies all safety factors to a number of *cycles:* ϕ_R is applied to the number of cycles N to resist failure in a nominal S–N curve, and γ_L to the number of cycles to be withstood in the service life. We may alternatively define nominal loads and resistances in terms of stresses, and find an equivalent set of factors γ'_L and ϕ'_R. Because damage is related to the b-th power of stresses, we may expect $\gamma'_L \approx \gamma_L^{1/b}$. For example, the typical values γ_L=10–20 in Figure 10 use b=8, suggesting corresponding factors γ'_L on stresses ranging from 1.33 to 1.45. These factors lie in a similar range as those of the Danish study (Ronold et al, 1994).

Summary and Conclusions

We have directly studied the fatigue reliability of two horizontal-axis wind turbines, one with rather dense load data (Turbine 1) and another with relatively sparse data (Turbine 2). We have also tried to infer similar results for a Danish machine, reported in a parallel fatigue reliability study (Ronold et al, 1994). Our findings include the following:

- To estimate fatigue damage, flapwise loads have been represented by their first three statistical moments across a range of wind conditions. The first two moments, μ_1 and μ_2, show similar trends for all 3 machines (Figures 2–3). Despite their rather different designs, Turbines 1 and 2 also show similar third moment μ_3 in Figure 4. This tends to support the goal of establishing a fairly general set of load distributions, at least for specific load components, HAWT designs, etc.

- Based on the moments $\mu_1 ... \mu_3$, we have introduced new "quadratic Weibull" load distribution models. By preserving μ_3, they more faithfully reflect the upper fractile of observed loads (e.g., Figure 1) than common two-moment models such as the Weibull or the lognormal. At the same time, they are rather simpler to implement than our earlier 4-moment models (e.g., Winterstein et al, 1994). This leads to particular savings when many fits are required; e.g., to estimate damage contributions over a range of wind speeds V and turbulence intensities I.

- The fatigue reliability is found to be notably affected by the choice of load distribution model. When lognormal, Weibull, and quadratic Weibull models are fit to the same 3 moments of loads data, typical failure probabilities for a 20-year life were found to differ by more than 5 orders of magnitude: from less than 10^{-6} to above 10^{-1}. This effect will grow with b; note that we choose here b=8, which is a relatively high value for metals but relatively low for many composites. Once an appropriate load distribution has been selected, this choice can be directly reflected in the fatigue design by seeking to preserve the nominal load L_{nom} in Eq. 16. Resulting load- and resistance

factors are then only mildly sensitive to the choice of load distribution (e.g., Figures 8–11).

- Because a broad range of load data is available for Turbine 1, its fatigue reliability is governed by the uncertainty in fatigue resistance R (e.g., uncertainty in S–N curve, Miner's rule, etc.). The required resistance factor ϕ_R—applied to the nominal S–N curve—is shown in Figure 9 to decrease steadily as the target p_f is lowered. This reflects that while the nominal resistance R_{nom} was somewhat conservatively set (2.3% fractile), still lower resistances must be designed against if we require still rarer failure events. In contrast, the load factor γ_L in this case is relatively flat, reflecting only the bias between the nominal "mean" load L_{nom} and the actual load most likely to cause failure.

- Because relatively sparse load data is available for Turbine 2, load and resistance uncertainties are found to be of comparable importance in this case. Thus the implied load and resistance factors in Figures 10–11 vary similarly over the range of p_f values reported: γ_L varies by about a factor of 2, and ϕ_R by about a factor of 3.

Acknowledgments

This program has been primarily supported by the Wind Energy Program of the U.S. Department of Energy, through a contract with Sandia National Laboratories. The authors especially thank Paul Veers and Herb Sutherland, of Sandia, for their many useful technical comments, and Tim McCoy of R. Lynette & Associates, for supplying the AWT-26 load data. Additional financial support for this work has been supplied by the Reliability of Marine Structures (RMS) program at Stanford University.

References

API, RP2A-LRFD (1993). *Recommended practice for planning, designing and constructing fixed offshore platforms—load and resistance factor design,* 1st edition, American Petroleum Institute.

Banon, H., R.G. Toro, E.R. Jefferys and R.S. De (1994). Development of reliability-based global design equations for TLPs. *Proc., 13th Intl. Offshore Mech. Arctic Eng. Symp.,* ASME, **II**, 335–343.

Coleman, C. and B. McNiff (1989). *Final report: dynamic response testing of the northwind 100 wind turbine,* Subcontractor Report, Solar Energy Research Institute, Golden, CO.

Jackson, K. (1992). Deriving fatigue design loads from field test data. *Proc., WindPower 92,* AWEA.

Kelley, N.D. (1995). A comparison of measured wind park load histories with the WISPER and WISPERX load spectra. *Proc., Wind Energy 1995,* ASME, SED **16**, 107–114.

Malcolm, D.J. (1990). Predictions of peak fatigue stresses in a Darrieus rotor wind turbine under turbulent winds. *Proc., 9th Wind Energy Symp.,* ASME, SED **9**, 125–135.

Mandell, J.F., R.M. Reed, D.D. Samborsky, and Q. Pan (1993). Fatigue performance of wind turbine blade composite materials. *Proc., 13th Wind Energy Symp.,* ASME, SED **14**.

McCoy, T.J. (1995). Load measurements on the AWT–26 prototype wind turbine. *Proc., Wind Energy 1995,* ASME, SED **16**, 281–290.

Ronold, K.O., J. Wedel-Heinen, C.J. Christensen, and E. Jorgensen (1994). Reliability-based calibration of partial safety factors for design of wind-turbine rotor blades against fatigue. *Proc., 5th European Wind Energy Conf.,* **II**, Thessaloniki, Greece, 927–933.

Veers, P.S. (1982). Blade fatigue life assessment with application to VAWTs. *J. Solar Energy Eng.,* **104**(2), 106–111.

Veers, P.S., S.R. Winterstein, and C.H. Lange (1993). FAROW: A tool for fatigue and reliability of wind turbines. *Proc., WindPower '93,* American Wind Energy Association.

Winterstein, S.R. and C.H. Lange (1995). Load models for fatigue reliability from limited data. *Proc., Wind Energy 1995,* ASME, SED **16**, 73–82.

Winterstein, S.R., C.H. Lange, and S. Kumar (1994). *FITTING: A subroutine to fit four moment probability distributions to data,* Rept. RMS–14, Rel. Marine Struc. Prog., Civil Eng. Dept., Stanford University.